Supporting Information

Atmospheric fate and impact of perfluorinated butanone and pentanone

Authors

Yangang Ren, François Bernard, Véronique Daële, Abdelwahid Mellouki *

Affiliations

Institut de Combustion Aérothermique, Réactivité et Environnement, Centre National de la Recherche Scientifique (ICARE-CNRS), Observatoire des Sciences de l'Univers en région Centre, CS 50060, 45071 cedex02, Orléans, France

Corresponding author

* mellouki@cnrs-orleans.fr

Journal: Environmental Science and Technology

Contents

Table S1: UV absorption cross sections (base e) of perfluoro-2-methyl-3-pentanone (PF-2M3P), 2-methyl-3-pentanone (2M3P) and perfluoro-3-methyl-2-butanone (PF-3M2B) measured in this work. The quoted uncertainties originated from 2 standard deviation (2σ) of the average of individual measurements.

Wavelength (nm)	Cross section (10^{-20} cm^2 $molecule^{-1}$)			Wavelength (nm)	Cross section (10^{-20} cm^2 $molecule^{-1}$)		
	2M3P	PF-2M3P	PF-3M2B		2M3P	PF-2M3P	PF-3M2B
220	0.13±0.06	0.08±0.02	0.17±0.08	311	2.34±0.12	6.00±0.30	3.04±0.13
221	0.16±0.08	0.09±0.03	0.16±0.07	312	2.11±0.12	5.91±0.30	2.97±0.12
222	0.17±0.08	0.05±0.03	0.16±0.07	313	1.87±0.12	5.81±0.33	2.89±0.12
223	0.15±0.09	0.02±0.02	0.15±0.06	314	1.66±0.11	5.77±0.37	2.77±0.11
224	0.20±0.10	0.06±0.02	0.15±0.06	315	1.45±0.10	5.68±0.36	2.64±0.11
225	0.20±0.10	0.05±0.03	0.14±0.6	316	1.27±0.10	5.60±0.40	2.51±0.10
226	0.19±0.10	0.03±0.02	0.13±0.06	317	1.10±0.10	5.50±0.39	2.38±0.10
227	0.23±0.13	0.05±0.02	0.13±0.05	318	0.94±0.10	5.33±0.41	2.27±0.09
228	0.23±0.13	0.09±0.03	0.13±0.06	319	0.82±0.09	5.14±0.39	2.19±0.10
229	0.26±0.13	0.09±0.03	0.13±0.05	320	0.68±0.08	4.89±0.36	2.11±0.10
230	0.29±0.10	0.04±0.02	0.14±0.07	321	0.57±0.06	4.65±0.36	2.05±0.09
231	0.30±0.12	0.08±0.03	0.14±0.06	322	0.48±0.06	4.39±0.28	2.00±0.09
232	0.34±0.11	0.10±0.04	0.14±0.06	323	0.39±0.05	4.19±0.9	1.94±0.07
233	0.37±0.10	0.07±0.04	0.14±0.05	324	0.33±0.03	4.01±0.26	1.88±0.08
234	0.41±0.08	0.10±0.03	0.14±0.05	325	0.27±0.03	3.89±0.28	1.80±0.07
235	0.45±0.10	0.13±0.05	0.15±0.09	326	0.23±0.05	3.78±0.25	1.71±0.08
236	0.49±0.09	0.11±0.06	0.16±0.09	327	0.18±0.04	3.70±0.25	1.60±0.08
237	0.54±0.09	0.14±0.08	0.16±0.08	328	0.14±0.03	3.61±0.21	1.48±0.08
238	0.62±0.10	0.14±0.08	0.17±0.08	329	0.12±0.03	3.53±0.20	1.36±0.07
239	0.67±0.09	0.16±0.8	0.19±0.08	330	0.10±0.03	3.43±0.21	1.20±0.07
240	0.74±0.08	0.17±0.09	0.20±0.07	331	0.08±0.03	3.28±019	1.10±0.07
241	0.81±0.09	0.19±0.10	0.21±0.09	332	0.06±0.03	3.11±0.15	1.01±0.07
242	0.90±0.08	0.20±0.10	0.22±0.08	333	0.05±0.03	2.88±0.18	0.94±0.08
243	1.00±0.08	0.23±0.12	0.25±0.80	334	0.04±0.03	2.66±0.14	0.88±0.07
244	1.09±0.09	0.24±0.12	0.26±0.06	335	0.04±0.02	2.41±0.14	0.83±0.07
245	1.19±0.09	0.29±0.12	0.28±0.07	336	0.03±0.02	2.18±0.14	0.77±0.07
246	1.29±0.09	0.28±0.12	0.31±0.07	337	0.03±0.02	1.99±0.15	0.72±0.07
247	1.42±0.08	0.35±0.11	0.33±0.07	338	0.02±0.02	1.82±0.14	0.72±0.04
248	1.54±0.10	0.38±0.11	0.37±0.06	339	0.01±0.01	1.68±0.15	0.66±0.03
249	1.67±0.11	0.41±0.12	0.40±0.07	340	0.01±0.01	1.60±0.13	0.60±0.03
250	1.80±0.10	0.45±0.11	0.44±0.07	341	0.01±0.01	1.51±0.13	0.54±0.03
251	1.95±0.10	0.50±0.10	0.48±0.07	342	0.02±0.01	1.49±0.15	0.47±0.03
252	2.10±0.10	0.57±0.12	0.52±0.07	343	0.03±0.02	1.44±0.14	0.41±0.04
253	2.26±0.11	0.61±0.12	0.56±0.07	344	0.03±0.02	1.35±0.16	0.34±0.03
254	2.43±0.12	0.66±0.11	0.61±0.06	345	0.01±0.01	1.27±0.18	0.29±0.03
255	2.61±0.12	0.74±0.14	0.67±0.08	346	0.02±0.01	1.15±0.15	0.24±0.03
256	2.79±0.13	0.79±0.15	0.72±0.08	347	0.02±0.01	1.01±0.14	0.20±0.04

257	2.95±0.12	0.84±0.15	0.77±0.08	348	0.02±0.01	0.87±0.16	0.17±0.02
258	3.14±0.13	0.95±0.15	0.83±0.07	349	0.02±0.01	0.74±0.17	0.14±0.03
259	3.36±0.14	1.01±0.20	0.89±0.07	350	0.02±0.02	0.60±0.15	0.11±0.03
260	3.58±0.14	1.06±0.26	0.96±0.08	351	0.02±0.02	0.50±0.12	0.09±0.03
261	3.78±0.15	1.18±0.21	1.03±0.07	352	0.02±0.02	0.41±0.18	0.07±0.03
262	3.99±0.17	1.27±0.21	1.10±0.07	353	0.03±0.02	0.31±0.13	0.07±0.02
263	4.22±0.15	1.36±0.19	1.18±0.08	354	0.02±0.02	0.25±0.11	0.05±0.02
264	4.43±0.16	1.46±0.1	1.25±0.08	355	0.02±0.02	0.20±0.10	0.04±0.02
265	4.64±0.16	1.57±0.0	1.33±0.07	356	0.02±0.02	0.17±0.09	0.04±0.02
266	4.87±0.19	1.67±0.19	1.41±0.07	357	0.02±0.02	0.13±0.08	0.04±0.02
267	5.09±0.19	1.81±0.13	1.50±0.07	358	0.03±0.02	0.12±0.07	0.03±0.02
268	5.30±0.19	1.92±0.20	1.59±0.07	359	0.02±0.02	0.09±0.08	0.03±0.02
269	5.52±0.21	2.04±0.19	1.67±0.07	360	0.02±0.02	0.08±0.08	0.02±0.02
270	5.70±0.21	2.16±0.19	1.78±0.08	361	0.02±0.02	0.09±0.09	0.02±0.01
271	5.85±0.22	2.30±0.19	1.87±0.07	362	0.03±0.02	0.08±0.07	0.02±0.02
272	6.02±0.24	2.46±0.19	1.96±0.09	363	0.03±0.02	0.06±0.03	0.02±0.02
273	6.18±0.25	2.60±0.22	2.04±0.09	364	0.02±0.02	0.04±0.04	0.02±0.02
274	6.33±0.26	2.74±0.21	2.13±0.08	365	0.03±0.02	0.05±0.05	0.02±0.02
275	6.46±0.25	2.92±0.21	2.22±0.08	366	0.03±0.02	0.07±0.03	0.02±0.02
276	6.59±0.28	3.03±0.20	2.30±0.10	367	0.02±0.02	0.06±0.0	0.02±0.02
277	6.68±0.28	3.20±0.22	2.37±0.08	368	0.03±0.02	0.05±0.04	0.02±0.02
278	6.76±0.29	3.32±0.22	2.46±0.10	369	0.02±0.02	0.02±0.02	0.02±0.02
279	6.84±0.30	3.49±0.20	2.54±0.09	370	0.03±0.03	0.05±0.03	0.02±0.02
280	6.91±0.30	3.66±0.20	2.63±0.09	371	0.03±0.03	0.06±0.03	0.02±0.02
281	7.00±0.30	3.82±0.21	2.70±0.10	372	0.03±0.03	0.04±0.02	0.02±0.02
282	7.06±0.32	3.99±0.25	2.78±0.10	373	0.03±0.03	0.04±0.02	0.02±0.02
283	6.88±0.28	4.14±0.25	2.84±0.10	374	0.03±0.03	0.06±0.03	0.02±0.02
284	6.99±0.28	4.28±0.20	2.91±0.10	375	0.04±0.03	0.04±0.03	0.02±0.02
285	6.96±0.29	4.49±0.29	2.96±0.12	376	0.02±0.02	0.04±0.02	0.03±0.02
286	6.91±0.28	4.61±0.30	3.03±0.2	377	0.04±0.03	0.05±0.03	0.02±0.02
287	6.88±0.28	4.73±0.26	3.09±0.12	378	0.04±0.03	0.05±0.03	0.03±0.02
288	6.85±0.28	4.86±0.27	3.15±0.13	379	0.03±0.03	0.02±0.02	0.03±0.02
289	6.82±0.28	4.97±0.30	3.19±0.13	380	0.03±0.03	0.05±0.02	0.03±0.02
290	6.75±0.28	5.16±0.27	3.23±0.14	381	0.05±0.03	0.05±0.03	0.02±0.02
291	6.65±0.27	5.27±0.27	3.27±0.14	382	0.05±0.03	0.04±0.03	0.03±0.02
292	6.51±0.25	5.44±0.27	3.28±0.14	383	0.03±0.03	0.07±0.03	0.03±0.02
293	6.34±0.24	5.58±0.26	3.29±0.14	384	0.04±0.03	0.04±0.02	0.03±0.02
294	6.16±0.24	5.73±0.27	3.31±0.14	385	0.05±0.03	0.07±0.03	0.02±0.02
295	5.99±0.23	5.86±0.32	3.35±0.14	386	0.04±0.03	0.06±0.03	0.03±0.02
296	5.82±0.22	5.92±0.27	3.38±0.15	387	0.05±0.04	0.05±0.03	0.03±0.02
297	5.67±0.21	6.00±0.29	3.39±0.16	388	0.05±0.04	0.04±0.02	0.03±0.02
298	5.52±0.21	6.05±0.31	3.43±0.17	389	0.05±0.04	0.04±0.02	0.02±0.02
299	5.34±0.19	6.11±0.29	3.46±0.16	390	0.04±0.04	0.06±0.02	0.02±0.02
300	5.14±0.19	6.15±0.27	3.48±0.15	391	0.06±0.04	0.04±0.02	0.02±0.02

301	4.89±0.19	6.23±0.25	3.47±0.15	392	0.05±0.05	0.04±0.02	0.02±0.02
302	4.61±0.19	6.34±0.32	3.44±0.14	393	0.05±0.04	0.07±0.03	0.02±0.02
303	4.33±0.17	6.41±0.29	3.39±0.14	394	0.05±0.05	0.03±0.02	0.02±0.02
304	4.04±0.16	6.47±0.29	3.33±0.14	395	0.06±0.05	0.02±0.02	0.02±0.02
305	3.76±0.16	6.50±0.28	3.28±0.13	396	0.05±0.05	0.03±0.02	0.01±0.02
306	3.51±0.17	6.52±0.31	3.24±0.13	397	0.07±0.05	0.04±0.02	0.02±0.02
307	3.28±0.15	6.48±0.30	3.21±0.12	398	0.06±0.05	0.04±0.02	0.02±0.02
308	3.03±0.14	6.37±0.32	3.19±0.13	399	0.06±0.05	0.04±0.02	0.02±0.02
309	2.81±0.14	6.26±0.32	3.15±0.12	400	0.06±0.05	0.05±0.03	0.02±0.02
310	2.59±0.13	6.11±0.32	3.09±0.13				

Table S2. TUV model parameters and photolysis rates of PF-2M3P, PF-3M2B and 2M3P based on the seasons of year from the TUV model using the quantum yield from this work.

47°N 1°E	Mar 22	Jun 22	Sept 22	Dec 22
O_3 total vertical column (DU)[a]	370	340	278	302
Cloud total optical depth [b]	18	22	20	31
Altitude of Cloud base (km)			5	
Altitude of Cloud top (km)			7	
$J_{PF\text{-}2M3P}$ ($\times 10^{-6}$ s^{-1}) 8am-8pm average	1.1±0.8	1.7±0.9	1.0±0.7	0.2±0.2
$J_{PF\text{-}2M3P}$ ($\times 10^{-6}$ s^{-1})12am-2pm average	2.1±0.2	2.8±0.2	2.0±0.1	0.4±0.1
J_{2M3P} ($\times 10^{-6}$ s^{-1})8am-8pm average	1.0±0.8	1.6±1.0	0.9±0.7	0.1±0.1
J_{2M3P} ($\times 10^{-6}$ s^{-1})12am-2pm average	2.1±0.2	2.8±0.2	1.8±0.1	0.3±0.1
$J_{PF\text{-}3M2B}$ ($\times 10^{-6}$ s^{-1})8am-9pm average	0.5±0.4	0.7±0.4	0.4±0.3	0.1±0.1
$J_{PF\text{-}3M2B}$ ($\times 10^{-6}$ s^{-1})12am-2pm average	0.9±0.1	1.2±0.1	0.8±0.1	0.2±0.1

[a] O_3 total vertical column data adapted from Veefkind et al. [3], [b] Cloud total optical depth adapted from NASA Earth Observations [2]

Table S3. Formation yield of identified products from the photolysis of perfluoro-2-methyl-3-pentanone (PF-2M3P).

PF-2M3P	COF_2 (%)	CF_3COF (%)	CO (%)	Fluorine balance (%)	Carbon balance (%)
3.4 m^3 outdoor chamber					
	196 ± 34	74 ± 8	160 ± 26	59 ± 8	84 ± 11
HELIOS outdoor chamber					
	191 ±24	75 ± 5	237 ± 22	57 ± 5	94 ±9
Weighted Average ±2σ[a]	193 ± 84	74 ±18	204± 68	57 ± 18	90 ± 28

[a] Weighted Average of each individual measurement: $Y_{av}=(w_1Y_1+ w_2Y_2 + \ldots)/(w_1+ w_2+\ldots)$, where $w=1/\sigma^2$, etc. The error is given by: $2\sigma_{av}=(\sigma_1^2+\sigma_2^2+ \ldots)^{0.5}$

Table S4. Lifetime, radiative efficiencies (RE) and GWPs (100 years) perfluoro-2-methyl-3-pentanone (PF-2M3P), perfluoro-3-methyl-2-butanone (PF-3M2B) and 2-methyl-3-pentanone (2M3P).

	Atmospheric Lifetime (days)	Radiative efficiencies (W m^{-2} ppb^{-1})		GWP_{100}[a]	Reference
		Well mixed[b]	Lifetime-adjusted[c]		
PF-2M3P	3-11	0.357	0.012-0.036	<0.21	This work
	7		0.03	<1	Hodnebrog, et al. [4]
	5.5		0.02	0.058	Díaz-de-Mera, et al. [5]
PF-3M2B	~13	~0.304	~0.036	~0.29	This work
2M3P	1-2	1.78×10^{-6}	$\leq4\times10^{-8}$	$\leq1.3\times10^{-7}$	This work

[a] GWP calculated for 100-year time horizon

[b] Calculated using the parameterization from Hodnebrog, et al. [4] for atmospherically well-mixed compounds.

[c] Calculated using the parameterization for short-lived compounds given in Hodnebrog, et al. [4]

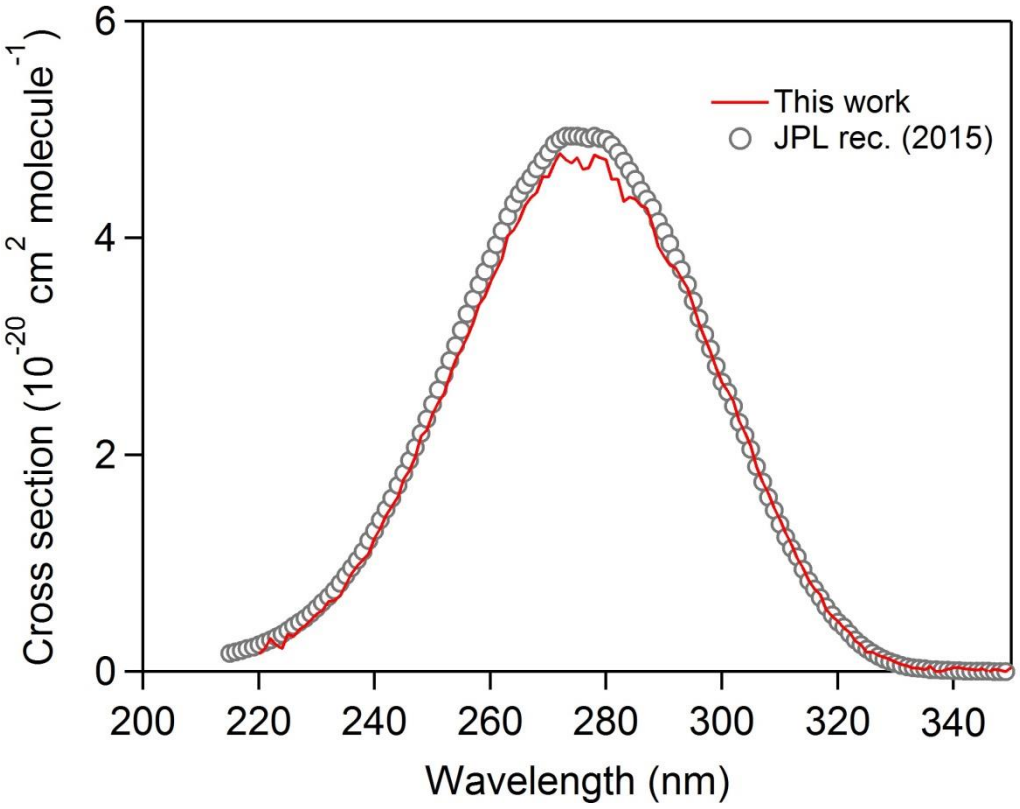

Figure S1. UV absorption spectra of acetone from this work and JPL recommendation (Burkholder et al., 2015)

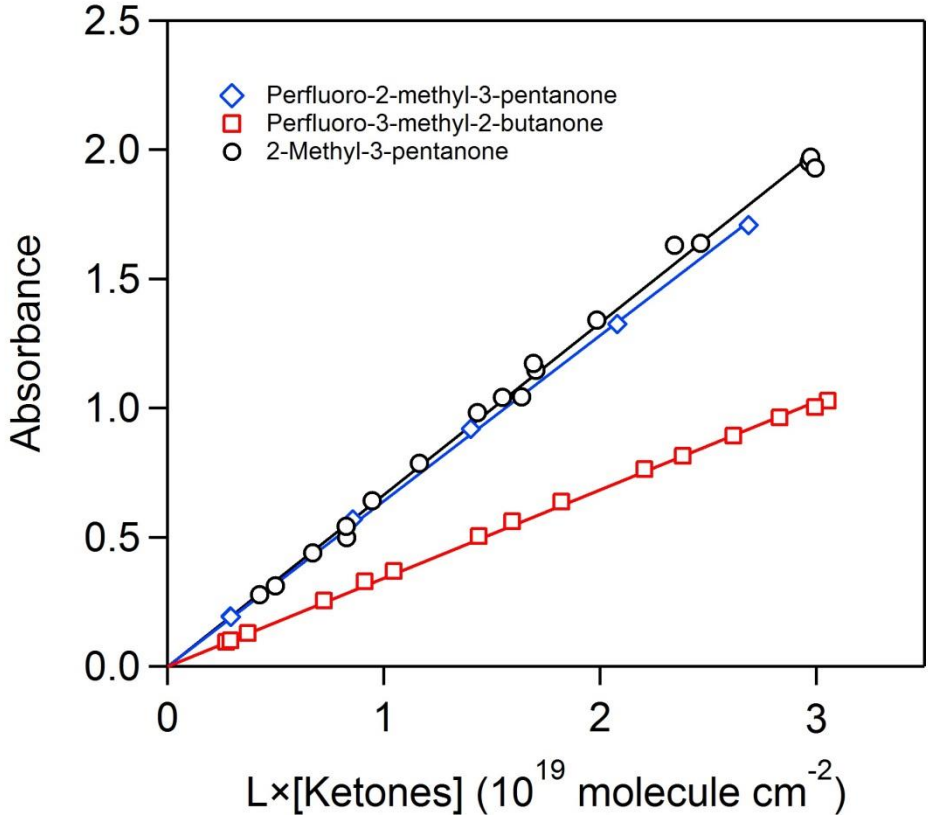

Figure S2. Beer's law fits from the UV-visible absorption spectra of perfluoro-2-methyl-3-pentanone (PF-2M3P), 2-methyl-3-pentanone (2M3P) and perfluoro-3-methyl-2-butanone (PF-3M2B) at the wavelength correpsonding to their maximum absorptions: 305 nm, 284 nm and 300 nm, respectively. Absorption path length (L) was 100 cm. The lines are linear least-squares fits to the combined data sets.

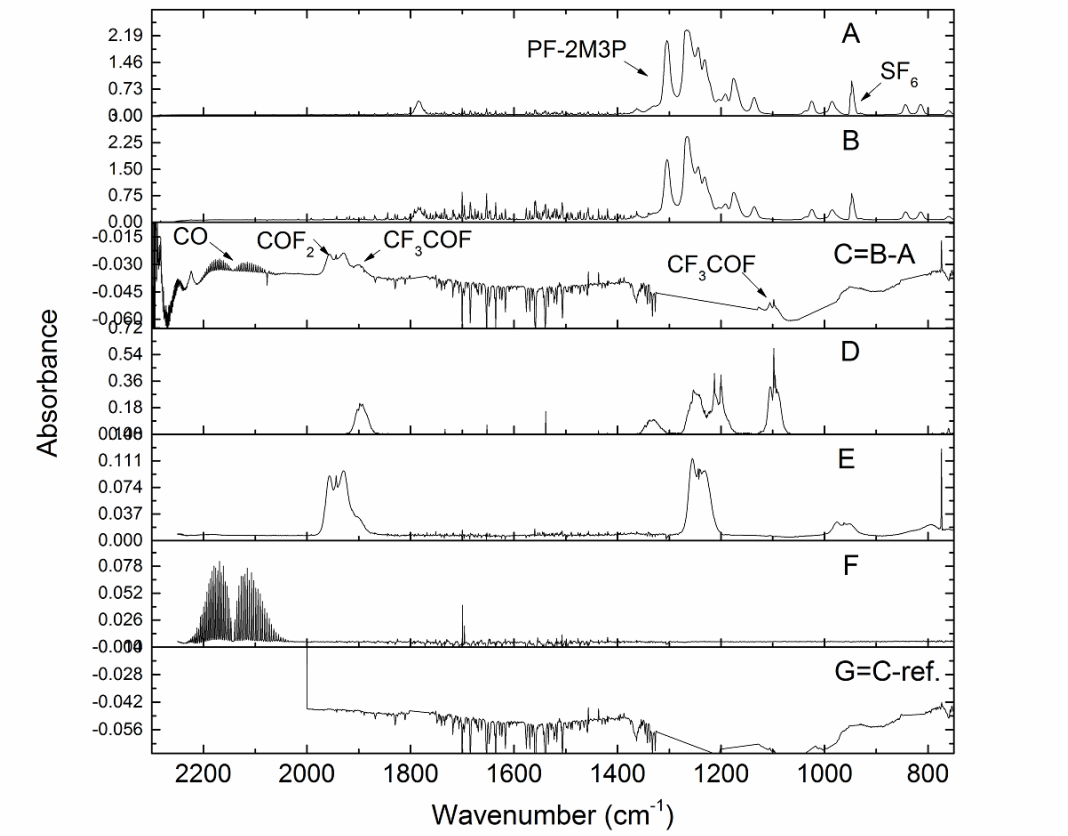

Figure S3. Photolysis of perfluoro-2-methyl-3-pentanone (PF-2M3P) conducted on on 19 September, 2013: FT-IR spectra (base *e*) recorded before (A) and after 4 hours exposure of PF-2M3P to sunlight (B). Panel C resulted from the subtraction of Panel B by Panel A. Reference spectra (base *e*) of $CF_3C(O)F$, COF_2 and CO are given in panel D, E and F, respectively. Residual spectrum subtracted from reactants and identified products are given in panel G.

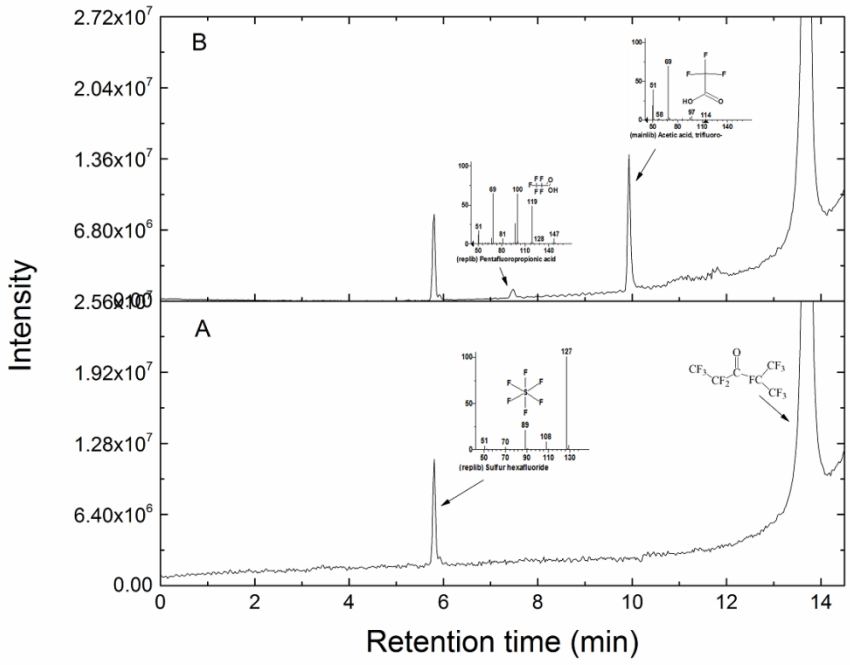

Figure S4. Chromatogram and MS spectrum from GC-MS analysis: before (A) and after (B) 4 hours exposure of PF-2M3P to sunlight.

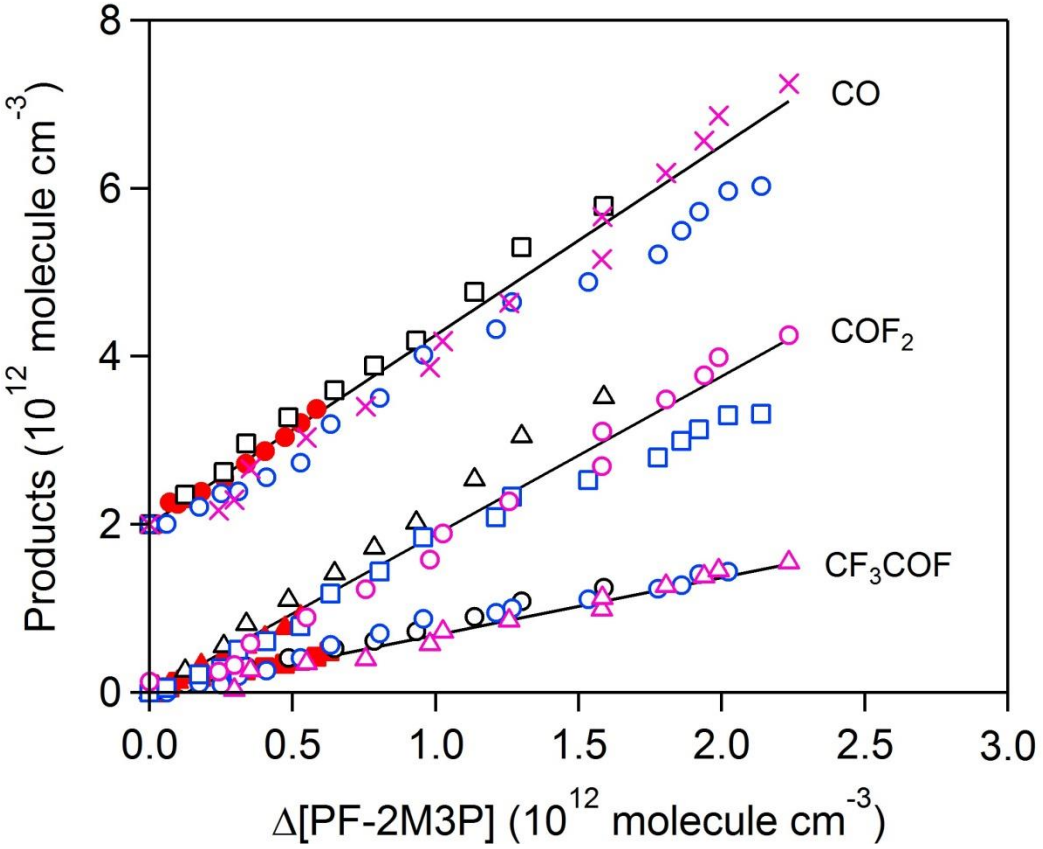

Figure S5. Formation of CO, COF_2 and CF_3COF versus the loss of perfluoro-2-methyl-3-pentanone (PF-2M3P) during the HELIOS photolysis experiments. The different colored symbols represent independent experimental measurements from this work as summarized in Table 1. The concentration of products was corrected from the dilution. The CO data were offset on the Y-axis by 2×10^{12} molecule cm^{-3} for clarity. The lines are the global linear least-squares fits of all the experimental data.

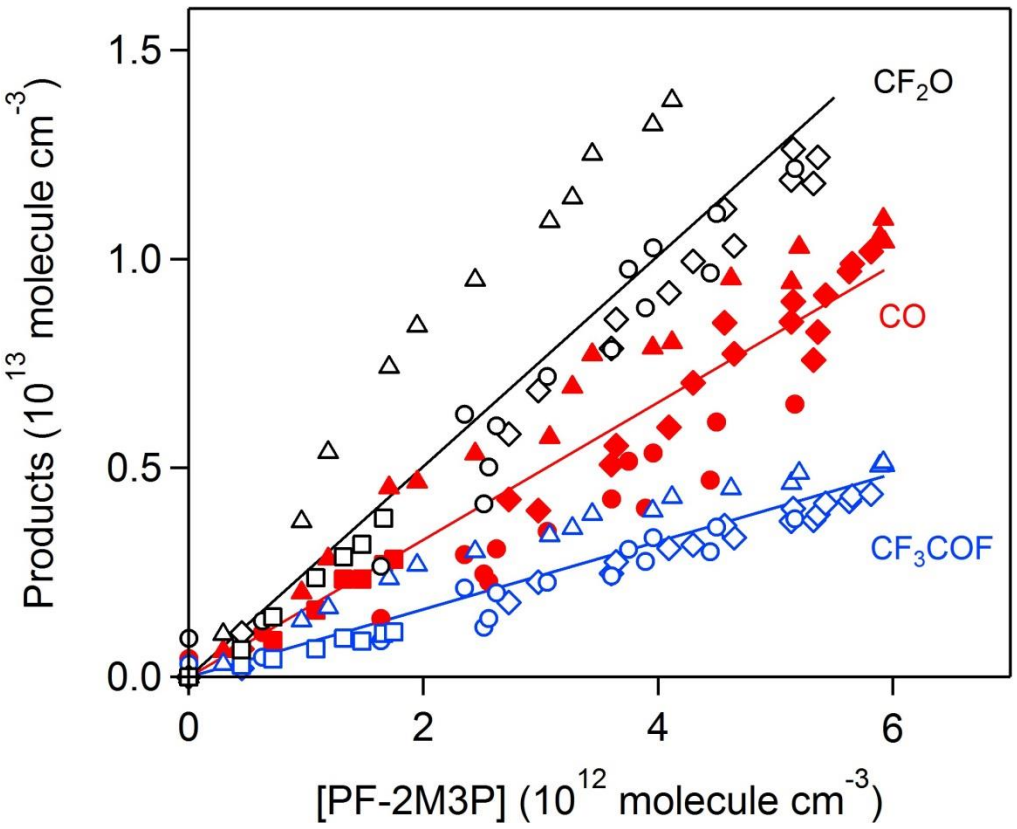

Figure S6. Formation of CF_2O, CO and CF_3COF versus the loss of perfluoro-2-methyl-3-pentanone (PF-2M3P) during the photolysis experiments obtained in the outdoor 3.4 m^3 chamber. The different colored symbols represent independent experimental measurements from this work as summarized in Table 1. The concentration of products was corrected from the dilution. The lines represent the global the linear least-squares fits of all the data.

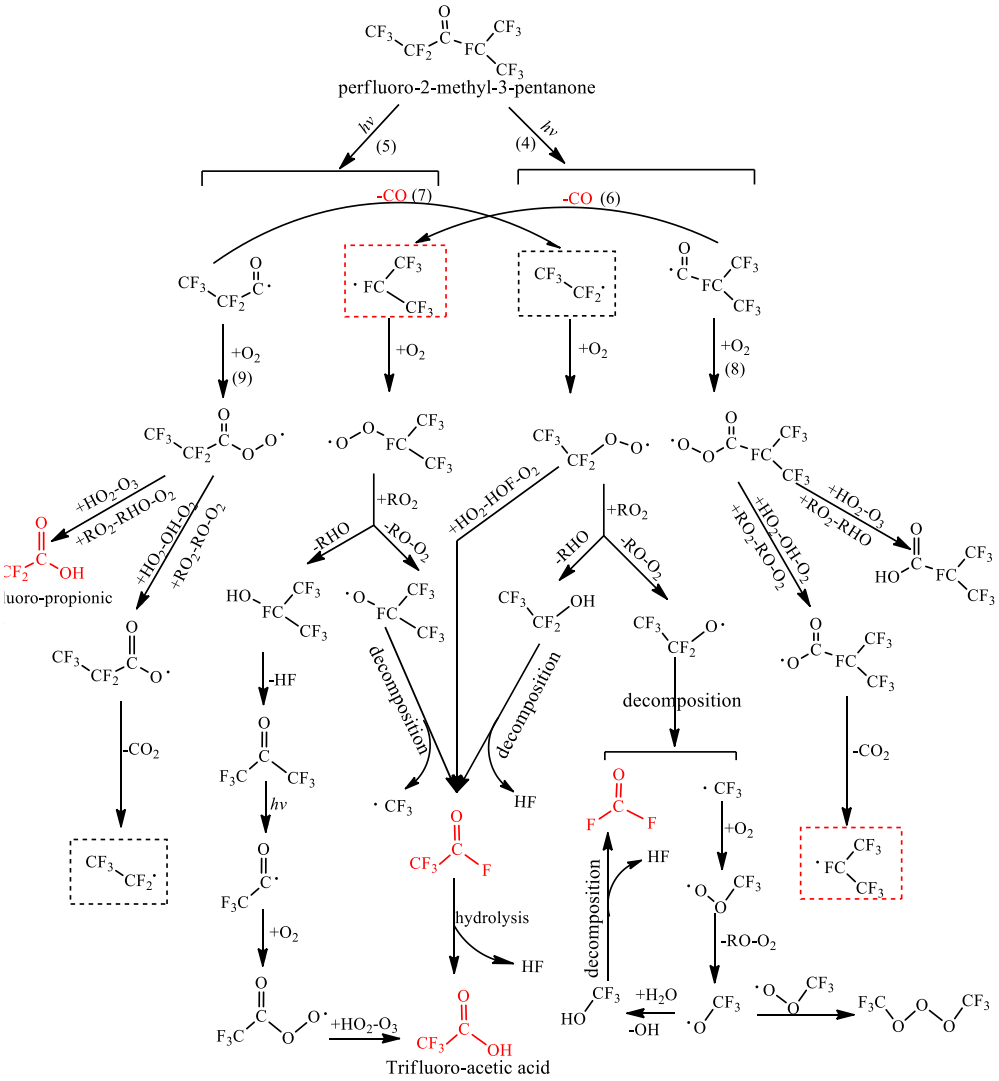

Figure S7. Photolysis of perfluoro-2-methyl-3-pentanone (PF-2M3P): proposed mechanism (adapated from Jackson, et al. [2]) leading to the formation of observed reaction products in the absence of NOx. Compounds in red represent products observed experimentally.

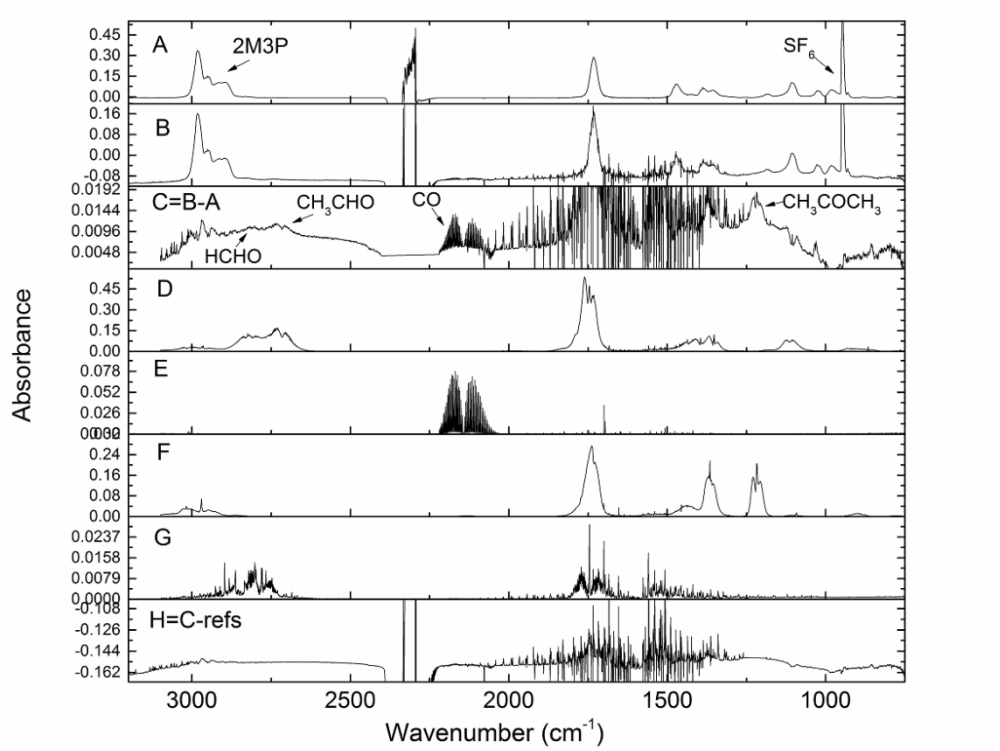

Figure S8. Photolysis of 2-methyl-3-pentanone (2M3P): FT-IR spectra (base e) recorded before (A) and after 6 hours exposure of MP to sunlight **(**B). Panel C shows the result of subtracting panel A from panel B**.** Reference spectra (base *e*) of CH_3CHO, CO, CH_3COCH_3 and HCHO are given in panel D, E, F and G. Residual spectrum subtracted from reactants and identified products is given in panel H.

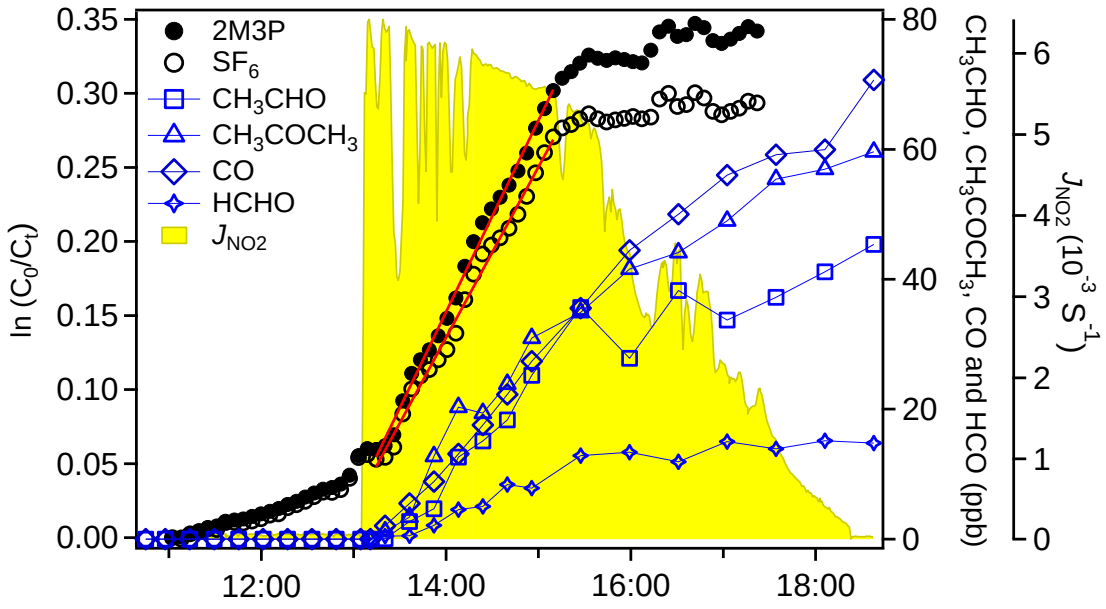

Figure S9. 2-Methyl-3-pentanone (2M3P) and its products during the photolysis experiment under natural irradiation in HELIOS (24 October 2013).

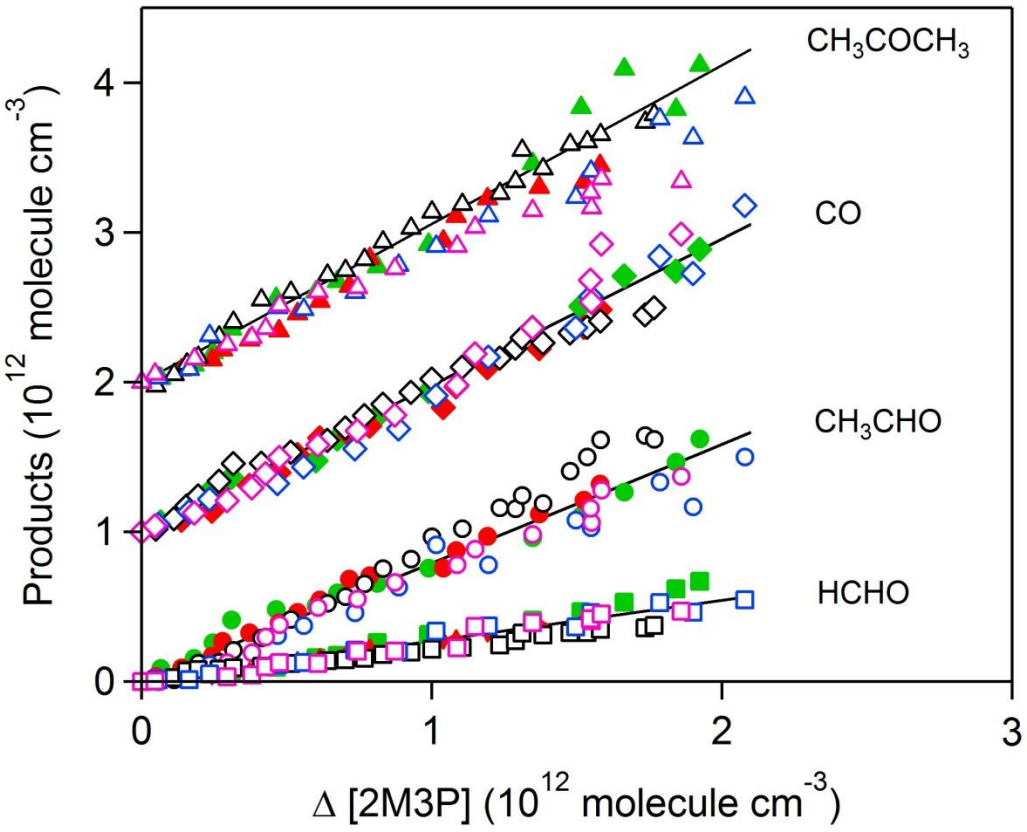

Figure S10. Formation of HCHO, CH_3CHO, CO and CH_3COCH_3 versus the loss of 2-methyl-3-pentanone (2M3P) during the photolysis experiments. The different colored symbols represent independent experimental measurements from this work as summarized in Table S4. CH_3COCH_3 and CO concentration data were offset on the Y-axis by 2×10^{12} and 1×10^{12} molecule cm^{-3}, respectively for clarity. The concentration of products was corrected to account for dilution (k_{SF6} under the irradiation condition) and their photolysis loss. The lines represent the global linear least-squares fits of all the data.

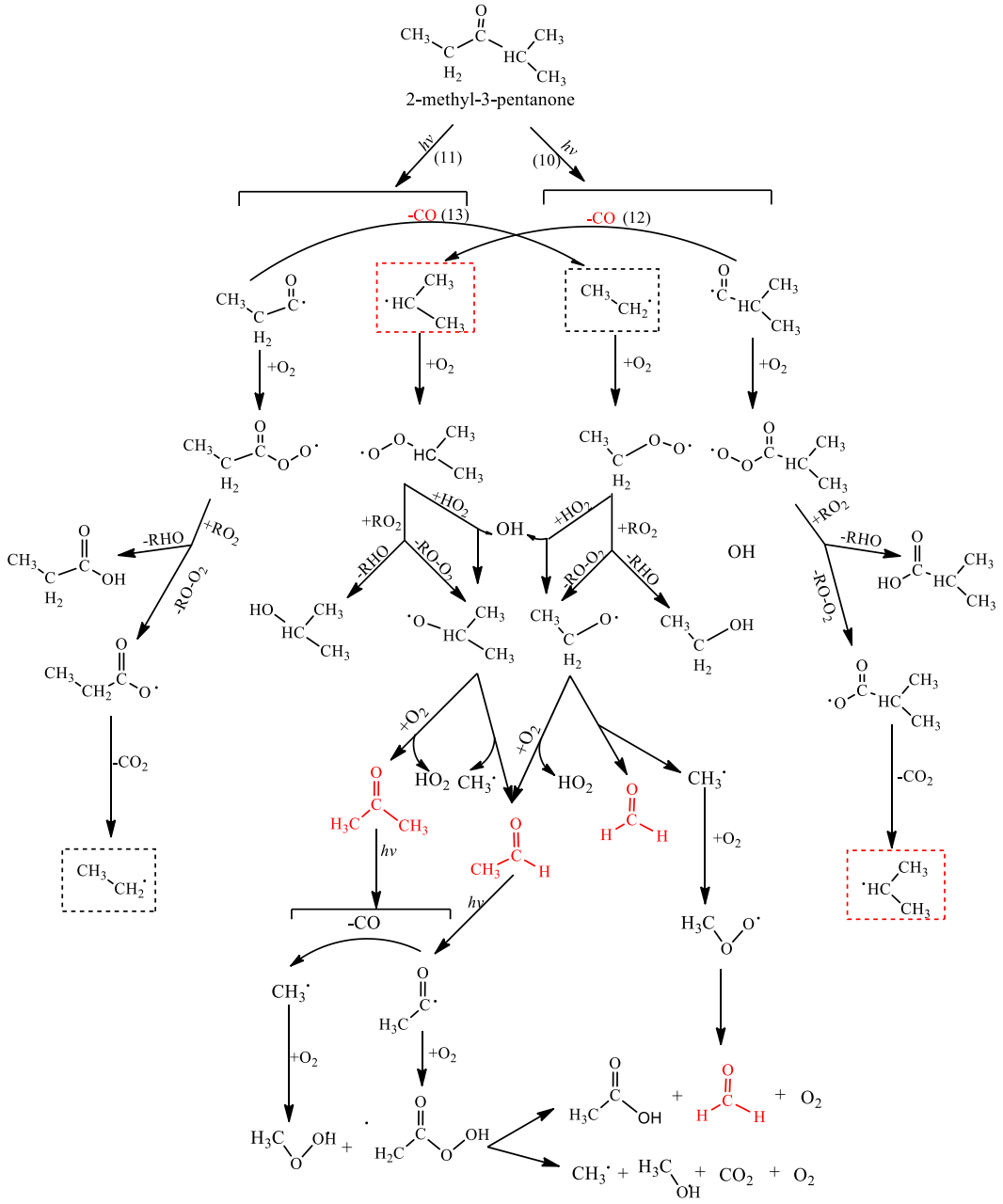

Figure S11. Photolysis of 2-methyl-3-pentanone (2M3P): proposed mechanistic pathways leading to the formation of observed products in the absence of NO_X. Compounds in red represent reaction products observed experimentally.

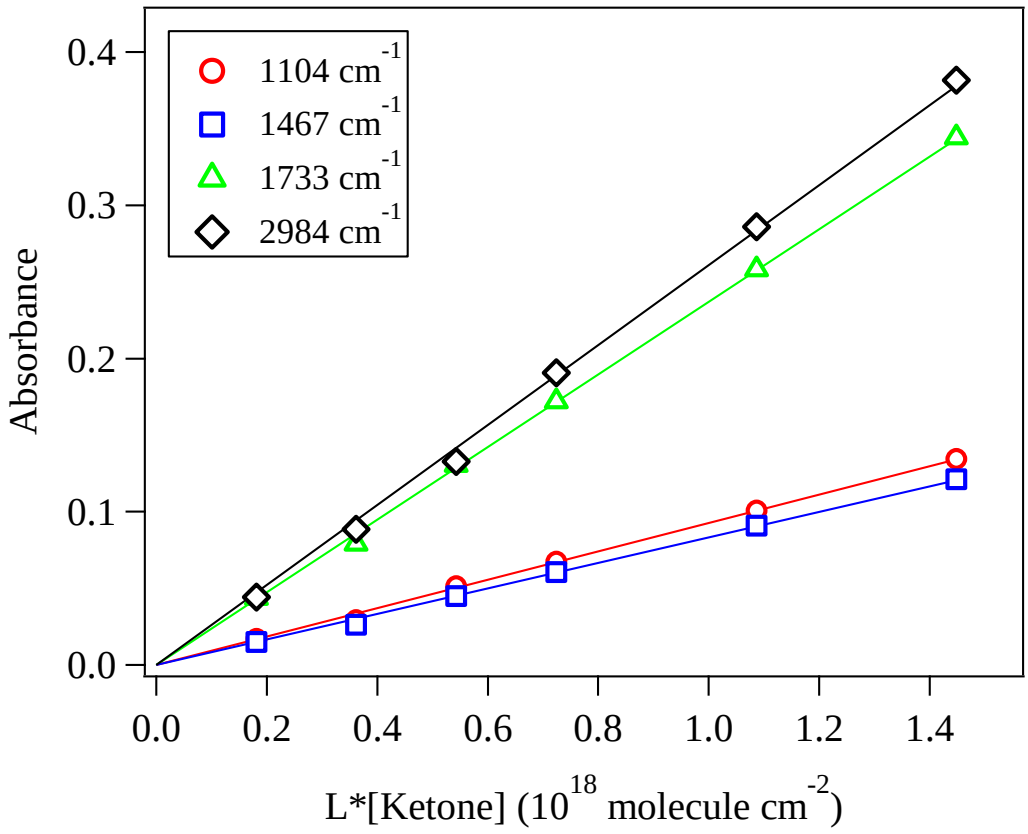

Figure S12. Infrared band strength data of 2-methyl-3-pentanone. The absorption cell path length (L) was 10 m. The lines are linear least-squares fits to the combined data sets.

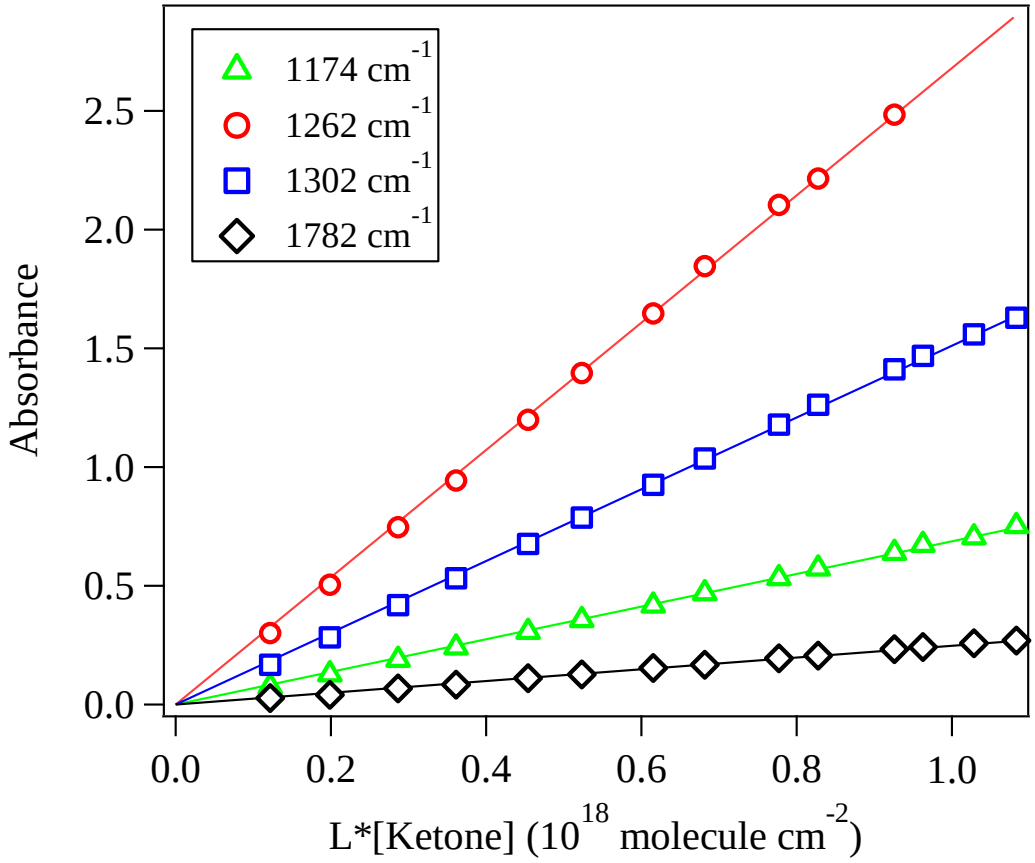

Figure S13. Infrared band strength data of perfluoro-2-methyl-3-pentanone. The absorption cell path length (L) was 10 m. The lines are linear least-squares fits to the combined data sets.

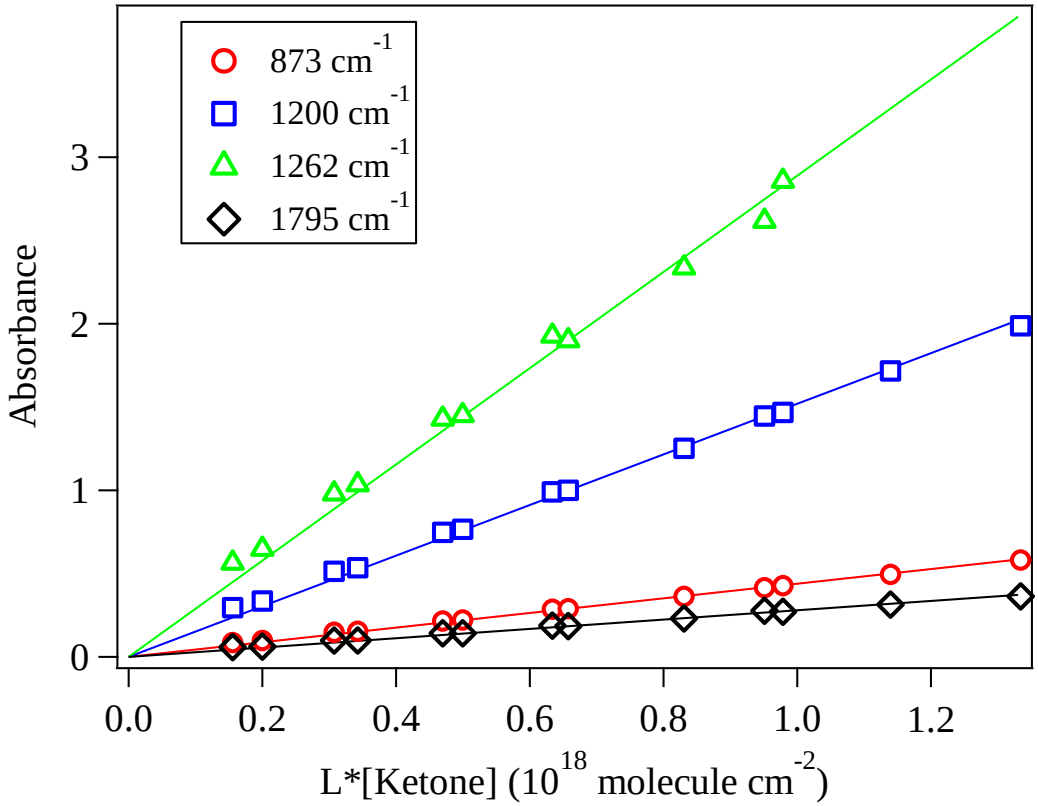

Figure S14. Infrared band strength data of perfluoro-3-methyl-2-butanone. The absorption cell path length (L) was 10 m. The lines are linear least-squares fits to the combined data sets.

References

(1) J. B. Burkholder; S. P. Sander; J. Abbatt; J. R. Barker; R. E. Huie; C. E. Kolb; M. J. Kurylo; V. L. Orkin; D. M. Wilmouth; Wine, P. H., Chemical Kinetics and Photochemical Data for Use in Atmospheric Studies, Evaluation No. 18. JPL Publication 15-10, J. P. L., Ed. Pasadena,, 2015.

(2) Jackson, D. A.; Young, C. J.; Hurley, M. D.; Wallington, T. J.; Mabury, S. A., Atmospheric Degradation of Perfluoro-2-methyl-3-pentanone: Photolysis, Hydrolysis and Hydration. *Environ. Sci. Technol.* **2011,** *45* (19), 8030-8036.

(3) Veefkind, J. P.; Haan, J. F. d.; Brinksma, E. J.; Kroon, M.; Levelt, P. F., Total ozone from the ozone monitoring instrument (OMI) using the DOAS technique. *IEEE Transactions on Geoscience and Remote Sensing* **2006,** *44* (5), 1239-1244.

(4) Hodnebrog, Ø.; Etminan, M.; Fuglestvedt, J. S.; Marston, G.; Myhre, G.; Nielsen, C. J.; Shine, K. P.; Wallington, T. J., Global warming potentials and radiative efficiencies of halocarbons and related compounds: A comprehensive review. *Rev. Geophys.* **2013,** *51* (2), 300-378.

(5) Díaz-de-Mera, Y.; Aranda, A.; Notario, A.; Rodriguez, A.; Rodriguez, D.; Bravo, I., Photolysis study of fluorinated ketones under natural sunlight conditions. *Phys. Chem. Chem. Phys.* **2015,** *17* (35), 22991-22998.